

## Analytical Chemistry

Two New Quinoline-Benzothiazole Blended 'Off-On' Type Fluorescent Probes Exclusively Detect  $\text{Cd}^{2+}$ Krishnendu Aich, Sangita Das, Saswati Gharami, Lakshman Patra, and Tapan Kumar Mondal<sup>\*[a]</sup>

In this paper, two new quinoline-benzothiazole based probes (QBTP1 and QBTP2) have been synthesized for the selective detection of  $\text{Cd}^{2+}$ . Both the probes showed selective 'Turn-On' emission change towards  $\text{Cd}^{2+}$ . Structure of QBTP1 was confirmed through its single crystal X-ray study. QBTP1 itself showed a weak emission band at 488 nm which upon addition of  $\text{Cd}^{2+}$  enhanced dramatically with a slight redshift to 507 nm. Consequently, weak cyan emission of QBTP1 changes to green which is easily observable through naked eyes. QBTP2 also showed almost similar fluorescence change upon addition of  $\text{Cd}^{2+}$  to that of QBTP1. The intramolecular charge transfer (ICT) and chelation enhanced fluorescence (CHEF) mechanisms may

play here the key role for this type of redshift of emission maximum and enhancement of fluorescence intensity respectively, upon addition of  $\text{Cd}^{2+}$  to the probes. Both the probes exclusively detect  $\text{Cd}^{2+}$  over any other cations tested. Most importantly, not a minute interference was observed by  $\text{Zn}^{2+}$  or  $\text{Hg}^{2+}$ . Capabilities of the probes to be used as portable kits for on-site detection of  $\text{Cd}^{2+}$  without using any expensive instrumental help was also shown here. Furthermore, the limit of detection of both the probes were found in the order of  $10^{-9}$  to  $10^{-10}$  M range which indicates the high sensitivity of the probes towards  $\text{Cd}^{2+}$ .

## Introduction

Cadmium has been recognized as a highly toxic heavy metal and is placed in the seventh position on the top twenty Hazardous Substances Priority List by the Agency for Toxic Substances and Disease Registry and the US Environmental Protection Agency (EPA).<sup>[1,2]</sup> There have been many reports on the toxicity of  $\text{Cd}^{2+}$  to the human kidney, lung, bone and nerve system, which resulted in many serious health problems such as renal dysfunction, calcium metabolism disorders and an increased incidence of certain forms of cancers.<sup>[3]</sup> The affordable level of cadmium in drinking water suggested by the WHO (World Health Organization) is 3 ppb to prevent the diseases held from cadmium toxicity.<sup>[4]</sup> In particular,  $\text{Cd}^{2+}$  can replace  $\text{Zn}^{2+}$  in many zinc enzymes, thereby impairing their catalytic activities.<sup>[5]</sup> The  $\text{Cd}^{2+}$ -uptake and carcinogenesis mechanisms are still insufficiently understood, mainly because of the lack of facile analytical methods for monitoring changes in the environmental and intracellular  $\text{Cd}^{2+}$  concentrations with high spatial and temporal reliability. Thus, the development of novel fluorescent sensors for  $\text{Cd}^{2+}$  has received considerable attention. However, it is still remaining a challenging task to design fluorescent switches for the exclusive detection of  $\text{Cd}^{2+}$ .  $\text{Zn}^{2+}$  or  $\text{Hg}^{2+}$  may interfere in the detection of  $\text{Cd}^{2+}$ .<sup>[6]</sup> So, it is being the main challenge to fabricate such type of fluorescent

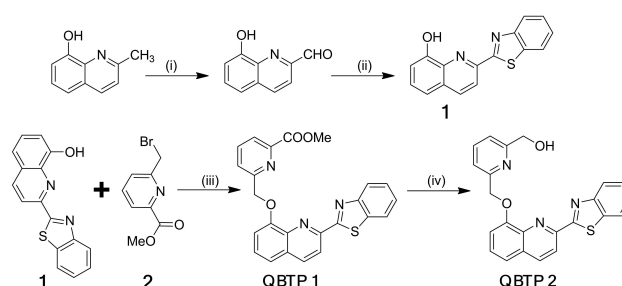
sensors which can be employed for detection of only  $\text{Cd}^{2+}$ . Therefore, tremendous efforts have been devoted for the development of fluorescence sensors which can detect  $\text{Cd}^{2+}$  without any interference from other bivalent ions.<sup>[7]</sup>

Keeping these factors in mind we have developed two new quinoline-benzothiazole blended fluorescent 'turn on' probes (QBTP1 and QBTP2), which can selectively detect  $\text{Cd}^{2+}$  in comparison to different guest analytes, especially  $\text{Zn}^{2+}$  and  $\text{Hg}^{2+}$ . The probing of  $\text{Cd}^{2+}$  was investigated by absorption, emission, <sup>1</sup>H NMR and HRMS spectroscopic techniques.

## Results and Discussion

## Synthesis of the probes (QBTP1 and QBTP2)

The synthetic scheme of the probes (QBTP1 & QBTP2) is shown in Scheme 1. Compound 1<sup>[7e]</sup> and compound 2<sup>[7c]</sup> are prepared



**Scheme 1.** Synthesis of the probes (QBTP1 and QBTP2). Reagents and conditions: (i)  $\text{SeO}_2$ , 1,4-dioxane, reflux, 6 h; (ii) 2-aminothiophenol, p-TSA, DMF,  $60^\circ - 70^\circ \text{C}$ , 12 h; (iii)  $\text{K}_2\text{CO}_3$ , DMF, TBAB, r.t., 6 h; (iv)  $\text{NaBH}_4$ ,  $\text{CH}_3\text{OH}$ , 2 h.

[a] K. Aich, S. Das, S. Gharami, L. Patra, T. K. Mondal  
Department of Chemistry, Jadavpur University, Jadavpur, Kolkata-700  
032, India  
E-mail: tapank.mondal@jadavpuruniversity.in

Supporting information for this article is available on the WWW under  
<https://doi.org/10.1002/slct.201901582>

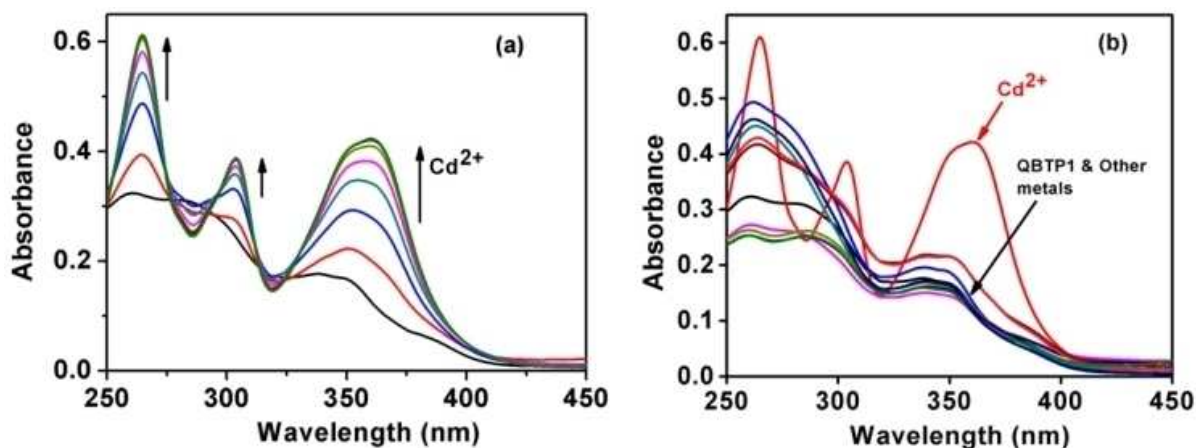


**Figure 1.** (a) Absorption spectral changes of QBTP1 (10  $\mu\text{M}$ ) upon gradual addition of  $\text{Cd}^{2+}$  (0 to 30  $\mu\text{M}$ ) in  $\text{CH}_3\text{OH}/\text{H}_2\text{O}$  (3/7, v/v) solution. (b) Absorption spectral changes of QBTP1 (10  $\mu\text{M}$ ) upon addition of different metal ions (30  $\mu\text{M}$ ) in  $\text{CH}_3\text{OH}/\text{H}_2\text{O}$  (3/7, v/v) solution.

according to the literature procedures. Condensation of compound 1 with compound 2 affords the probe QBTP1 as white solid. Reduction of QBTP1 using sodium borohydride yields another probe QBTP2. Detailed synthetic procedures of these probes are given in the experimental section. Chemical structures of QBTP1 & QBTP2 are well characterised through  $^1\text{H}$ NMR,  $^{13}\text{C}$ NMR and HRMS spectroscopic techniques (Figure S1-S8, SI). In addition, structure of QBTP1 is also confirmed by single crystal X-ray study.

### UV-Vis studies of QBTP1

The objective of preparation of such kind of ICT-CHEF based probes is to get a beautiful spectrum both in emission and in absorbance after interaction with the guest cations. Now the cation binding properties of the probes (QBTP1 and QBTP2) was examined by employing aqueous solutions of different cations ( $\text{Na}^+$ ,  $\text{K}^+$ ,  $\text{Ca}^{2+}$ ,  $\text{Ni}^{2+}$ ,  $\text{Mn}^{2+}$ ,  $\text{Zn}^{2+}$ ,  $\text{Cd}^{2+}$ ,  $\text{Cu}^{2+}$ ,  $\text{Fe}^{3+}$ ,  $\text{Cr}^{3+}$ ,  $\text{Pb}^{2+}$ ,  $\text{Al}^{3+}$ ,  $\text{Hg}^{2+}$ ) as their perchlorate salts. As shown in Figure 1a, the UV-Vis spectrum of QBTP1 in absence of any guest analytes, exhibits three absorption bands centred at 260 nm, 282 nm and 350 nm respectively. Upon addition of  $\text{Cd}^{2+}$  (0 to 1.7 equiv.), the absorption spectrum of QBTP1 exhibits a beautiful cascade type of spectrum. Upon incremental addition of  $\text{Cd}^{2+}$  in the assay condition the peak at 350 nm slightly red shifted along with a noticeably increment in the absorbance intensity, observed at 360 nm. Four isobestic points were found at 276, 292, 313 and 325 nm respectively. This is an interesting feature of UV-Vis spectroscopy by which we can detect  $\text{Cd}^{2+}$ , consequently without implementation of any other instrumental technique. By simply observing we can easily establish that  $\text{Cd}^{2+}$  is strongly associated with QBTP1. No other guest analyte ( $\text{Na}^+$ ,  $\text{K}^+$ ,  $\text{Ca}^{2+}$ ,  $\text{Ni}^{2+}$ ,  $\text{Mn}^{2+}$ ,  $\text{Zn}^{2+}$ ,  $\text{Cu}^{2+}$ ,  $\text{Fe}^{3+}$ ,  $\text{Cr}^{3+}$ ,  $\text{Pb}^{2+}$ ,  $\text{Al}^{3+}$ ,  $\text{Hg}^{2+}$ ) of interest can perturb any notable deformation in UV-vis profile of QBTP1 (Figure 1b). Even the higher concentration of  $\text{Zn}^{2+}$  does not lead to any significant distortion.

### UV-vis study of QBTP2

The UV-vis titrations of QBTP2 (10  $\mu\text{M}$ ) were conducted in  $\text{MeOH}/\text{H}_2\text{O}$  (1/9, v/v, 1 mM HEPES buffer,  $\text{pH}=7.2$ ) solutions. In the absorption spectra, QBTP2 (10  $\mu\text{M}$ ) itself exhibits two absorption bands at 265 and 345 nm, and no peak at 360 nm indicating the probe is stable in this situation (Figure 2a). Now, with frequent addition of  $\text{Cd}^{2+}$  into the solution of QBTP2, a new peak arises at 360 nm, whereas a decrease at 322 nm was observed. Consequently two well defined isobestic points were come into view at 342 and 381 nm respectively. Now this entire observation explains the change in the UV-vis spectrum is due to the combination of complexation of QBTP2 with  $\text{Cd}^{2+}$  which ultimately increased the ICT efficiency of the system. Now upon addition of different guest metal ions ( $\text{Na}^+$ ,  $\text{K}^+$ ,  $\text{Ca}^{2+}$ ,  $\text{Ni}^{2+}$ ,  $\text{Mn}^{2+}$ ,  $\text{Zn}^{2+}$ ,  $\text{Cu}^{2+}$ ,  $\text{Fe}^{3+}$ ,  $\text{Cr}^{3+}$ ,  $\text{Pb}^{2+}$ ,  $\text{Al}^{3+}$  and  $\text{Hg}^{2+}$ ) into the solution of QBTP2, there was no obvious change in the UV-vis spectrum observed (Figure 2b). From here it is quite easy to interpret that the probe can surely detects  $\text{Cd}^{2+}$  in comparison to different guest cations.

### Emission study of QBTP1

The emission spectra of QBTP1 was studied in  $\text{MeOH}/\text{H}_2\text{O}$  (3/7, v/v, 10 mM HEPES buffer,  $\text{pH}=7.2$ ) solution in presence of various metal cations. In Fig 3, we can see that the fluorescence spectrum of the free probe (QBTP1, 10  $\mu\text{M}$ ) exhibits a low emission at 488 nm upon excitation at 360 nm. Upon addition of  $\text{Cd}^{2+}$ , the peak at 488 nm is red shifted to 507 nm with a swift "turn-on" enhancement in the emission intensity. Such a red shift is attributed to a good opportunity for exclusive fluorescent  $\text{Cd}^{2+}$  detection using this new probe. This red shift of  $\sim 19$  nm in the emission spectra of QBTP1 strongly indicates that the nitrogen atoms of the quinoline and pyridine platforms may strongly coordinated with  $\text{Cd}^{2+}$ , as because the nitrogen atom of quinoline moiety has a strong affinity towards  $\text{Cd}^{2+}$ . This  $\text{Cd}^{2+}$  induced chelation ultimately enhanced ICT

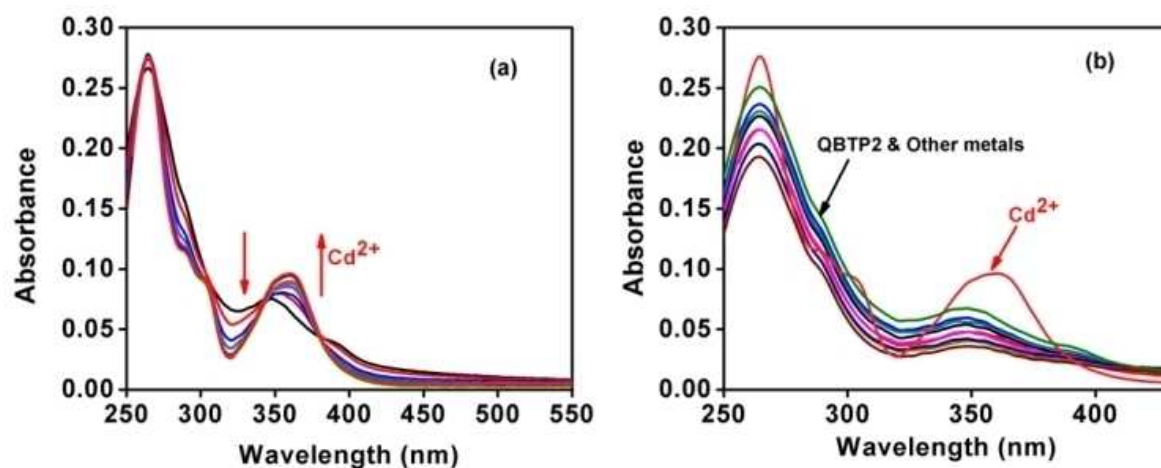


**Figure 2.** (a) Absorption spectral changes of QBTP2 (10  $\mu\text{M}$ ) upon gradual addition of  $\text{Cd}^{2+}$  (0 to 30  $\mu\text{M}$ ) in  $\text{CH}_3\text{OH}/\text{H}_2\text{O}$  (1/9, v/v) solution. (b) Absorption spectral changes of QBTP2 (10  $\mu\text{M}$ ) upon addition of different metal ions (30  $\mu\text{M}$ ) in  $\text{CH}_3\text{OH}/\text{H}_2\text{O}$  (1/9, v/v) solution.

efficiency of the system. This entire phenomenon suggests a chelation-elicited effective ICT mechanism plays the key mechanism for this kind of observation. Consequently, a distinct fluorescence colour change was noticed from cyan to light-green (Figure 3, inset). The emission intensity of QBTP1

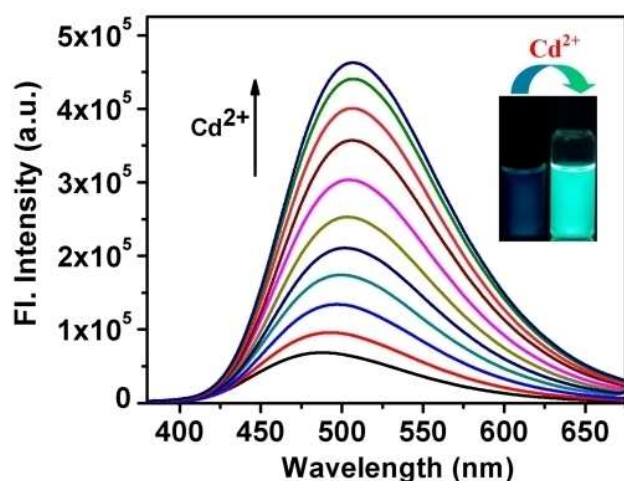


**Figure 3.** Change of emission spectra of QBTP1 (10  $\mu\text{M}$ ) upon gradual addition of  $\text{Cd}^{2+}$  (0 to 30  $\mu\text{M}$ ). Inset: Photograph showing the visible color change of QBTP1 before and after addition of  $\text{Cd}^{2+}$  (20  $\mu\text{M}$ ) under UV light.

was also studied in presence of other metal cations such as  $\text{Na}^+$ ,  $\text{K}^+$ ,  $\text{Ca}^{2+}$ ,  $\text{Ni}^{2+}$ ,  $\text{Mn}^{2+}$ ,  $\text{Zn}^{2+}$ ,  $\text{Cu}^{2+}$ ,  $\text{Fe}^{3+}$ ,  $\text{Cr}^{3+}$ ,  $\text{Pb}^{2+}$ ,  $\text{Al}^{3+}$ ,  $\text{Hg}^{2+}$  but no significant changes were noticed for any of the other metal ions (Fig S9, SI).

It was observed that up to 10  $\mu\text{M}$  the linearity maintained, further any addition of  $\text{Cd}^{2+}$  a plateau was reached in the spectra, indicates the saturation takes place. The emission intensity of QBTP1 exhibits a good linear curve of fitness with added  $\text{Cd}^{2+}$  concentration (0 to 17.8  $\mu\text{M}$ , Fig S11, SI) with a  $R^2$

value of 0.9985. Now in order to estimate the stoichiometry of the  $\text{Cd}^{2+}$ -complex, job's plot was executed. The maxima of the plot shows the mole fraction at 0.5 for  $\text{Cd}^{2+}$ , which implies to the 1:1 complex formation of QBTP1 and  $\text{Cd}^{2+}$  (SI, Figure S12). The HRMS spectrum of QBTP1- $\text{Cd}^{2+}$  also supports this fact by exhibiting a peak at  $m/z$  610.9217 (Figure S4, SI). Moreover, the detection limit of the probe for  $\text{Cd}^{2+}$  was determined from the fluorescence spectral change, and it was found to be  $3.52 \times 10^{-10}$  M, using the equation  $\text{DL} = K \times \text{Sb}_1 / S$ , where  $K=3$ ,  $\text{Sb}_1$  is the standard deviation of the blank solution and  $S$  is the slope of the calibration curve<sup>[8]</sup> (Figure S13, SI). The association constant was also calculated to be  $3.17 \times 10^4 \text{ M}^{-1}$  according to the emission spectral titration data by Bensi-Hildebrand equation (Figure S14, SI) suggesting that the complex is stable enough. Moreover upon addition of above mentioned guest cations, even in excess amount does not led to any significant change. Especially upon addition of  $\text{Zn}^{2+}$  and  $\text{Hg}^{2+}$ , no changes in the emission spectrum were observed indicating there is no coordination between  $\text{Zn}^{2+}$  and  $\text{Hg}^{2+}$  with QBTP1.

#### Emission study of QBTP2

The emission behaviour of QBTP2 was also investigated in the same mixed solvent as that of in QBTP1 (MeOH/ $\text{H}_2\text{O}$ , 1/9, v/v, 10 mM HEPES buffer, pH=7.2) solution. Free receptor (QBTP2) showed a weak band at 490 nm ( $\lambda_{\text{ex}} = 360$  nm). Upon gradual addition of different guest metal ions, only  $\text{Cd}^{2+}$  can induce a significant fluorescence change with a quantum yield of 0.22 (the Q.Y of QBTP2 itself was 0.15), thus exhibiting an efficient ICT-CHEF based behaviour. Various other metal ions show almost negligible changes in PL intensity of QBTP2 (Fig S15, SI). By observing the initial actions of the probe QBTP2 towards  $\text{Cd}^{2+}$ , we are interested to see the quantitative behaviour of  $\text{Cd}^{2+}$  for QBTP2. As shown in figure 4, upon incremental addition of  $\text{Cd}^{2+}$  to the solution of QBTP2, the initial peak at 490 nm was red-shifted to 510 nm, along with a 20-fold "turn-on" emission enhancement. Incremental addition of  $\text{Cd}^{2+}$  to

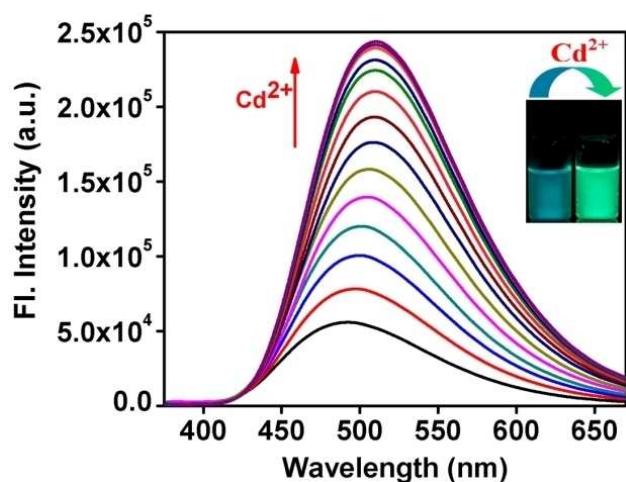


**Figure 4.** Change of emission spectra of QBTP2 (10  $\mu\text{M}$ ) upon gradual addition of  $\text{Cd}^{2+}$  (0 to 30  $\mu\text{M}$ ). Inset: Photograph showing the visible color change of QBTP2 before and after addition of  $\text{Cd}^{2+}$  (20  $\mu\text{M}$ ) under UV light.

the solution of QBTP2 resulted in a prompt dramatic color change from cyan to bright green (Figure 4, inset). The evident color change could be determined by naked eye. The emission intensity of QBTP2 at 510 nm exhibits a good linear relationship with added  $\text{Cd}^{2+}$  concentration. Upon incremental addition of  $\text{Cd}^{2+}$ , the fluorescence emission maximum at 510 nm linearly increased with the amount of  $\text{Cd}^{2+}$  added in between 0 to 20.6  $\mu\text{M}$  ( $R^2 = 0.9904$ ) and reached a plateau when the concentration of  $\text{Cd}^{2+}$  was 1 equiv. (Fig S17, SI). The Job's method monitored by fluorescence intensities was applied to examine the stoichiometry of the QBTP2: $\text{Cd}^{2+}$  complex, indicating a 1:1 stoichiometry of QBTP2 to  $\text{Cd}^{2+}$  in the complex (Fig S18, SI). The HRMS spectrum for QBTP2- $\text{Cd}^{2+}$  was also recorded which supports the 1:1 complexation by showing a peak at  $m/z$  582.9417 (Figure S8, SI). The limit of detection (LOD) was determined by means of fluorescence titration and it is found to be  $4.83 \times 10^{-9}$  M, based on the equation,  $\text{LOD} = 3\sigma/s$ , where  $\sigma$  is the standard deviation of blank measurements, and  $s$  is the

slope between fluorescence intensity versus  $\text{Cd}^{2+}$  concentration (Fig S19, SI). The association constant was calculated to be  $1.60 \times 10^4 \text{ M}^{-1}$  (Fig S20, SI) according to the spectral titration data by Bensi-Hildebrand equation.

### Competition Experiment

Now the selectivity and sensitivity are the two very important properties to evaluate the efficiency of any receptor. Subsequently in order to prove the strong selectivity of the probes towards  $\text{Cd}^{2+}$  over other important guest cations (especially towards  $\text{Zn}^{2+}$ ) were studied by means of fluorescence studies. So a competitive study was then executed by measuring the fluorescence intensity of both the probes (10  $\mu\text{M}$ ) in presence of other metal ions (20  $\mu\text{M}$ ) in order to study the specific selectivity of QBTP1 and QBTP2. It is eminent from the experiment that both the probes have a strong and specific affinity towards  $\text{Cd}^{2+}$  (Figure 5a and 5b) and the presence of other metal cations do not affect it in any other way. Thus the competition experiment established that the probes (QBTP1 and QBTP2) displayed a foremost and distinct response only towards  $\text{Cd}^{2+}$  without any interference.

### pH study

The acid-base titration experiment of QBTP1 was carried out and it was revealed from the titration that this fluorescent probe does not undergo significant changes in emission intensity at 507 nm with varying pH (Fig S21a, SI). Now upon addition of  $\text{Cd}^{2+}$  into the solution of QBTP1, the emission intensity increases sharply with increasing pH. Thus we can say that QBTP1 is entirely capable in detecting  $\text{Cd}^{2+}$  within the pH range of 2.2-7.2. But on further increase of pH, the emission intensity of the probe decreases sharply thereby indicating that in basic region ( $\text{pH} = 8.5-11.4$ ), QBTP1 is not able to detect  $\text{Cd}^{2+}$ . Similarly, it was found that the second probe, QBTP2 also showed the same emission intensity change at 510 nm with varying pH on addition of  $\text{Cd}^{2+}$  into it (Fig S21b, SI). So the above experiment unveils the fact that both QBTP1 and QBTP2

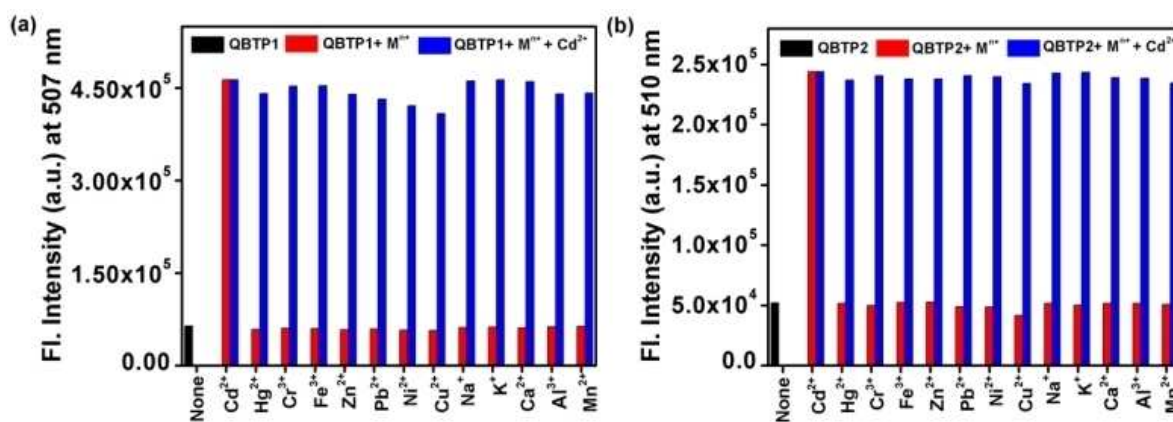


**Figure 5.** Bar diagram illustration of the relative emission intensity of (a) QBTP1 and (b) QBTP2 upon addition of various metals (10  $\mu\text{M}$ ) (red bars) and  $\text{Cd}^{2+}$  (20  $\mu\text{M}$ ) in presence of other metal ions (blue bars).



can be used as extremely effective sensors for  $\text{Cd}^{2+}$  in near neutral pH ( $\text{pH} = 7.2$ ).

### Reversibility study

We have studied the reversibility of both QBTP1 and QBTP2 with the help of  $\text{Na}_2\text{EDTA}$  solution. To confirm whether the complexation processes are reversible or not, emission studies were carried out towards both QBTP1- $\text{Cd}^{2+}$  and QBTP2- $\text{Cd}^{2+}$  complexes with  $\text{Na}_2\text{EDTA}$  solution. From this titration experiment, it is observed that the emission intensity gets quenched and almost reverted back to the original intensity of QBTP1 and QBTP2 respectively suggesting the decomplexation of both QBTP1 and QBTP2 by the formation of  $\text{Cd}^{2+}$ -EDTA adduct (Fig S10 and S16, SI). Thus, both the probes can be reused for the detection of  $\text{Cd}^{2+}$  after subsequent treatment with  $\text{Na}_2\text{EDTA}$  solution indicating the potentiality of the probes.

### Detection of $\text{Cd}^{2+}$ using test-kit

In order to demonstrate some potential applications of these two probes (QBTP1 and QBTP2), we have executed an effective analysis known as dipstick method with both of them. Through this experiment, one can prove that the sensing property of a probe towards a particular metal ion can be displayed in solid state too. This dipstick experiment can provide some important qualitative information on detecting a particular metal ion without the aid of any real instruments which is of huge importance to researchers. So to perform this experiment, few TLC plates were prepared and they are immersed into both QBTP1 and QBTP2 solution ( $2 \times 10^{-4}$  M) in MeOH and then kept aside for a few minutes to evaporate the solvent. Then the TLC plates are immersed into  $\text{Cd}^{2+}$  ( $2 \times 10^{-3}$  M) solution and then the solvent was again evaporated in order to dry those plates. During this experiment, one can easily study the detection of  $\text{Cd}^{2+}$  by their naked eye too. In case of QBTP1, the colour of the TLC plates show the change from dark blue to deep green fluorescence whereas in case of QBTP2, the fluorescence change is slightly different by showing the color change from deep cyan blue to sab green in presence of  $\text{Cd}^{2+}$  in the UV chamber (Figure 6). So it can be concluded that both the probes, QBTP1 and QBTP2 can be used as a portable fluorescence kit which shows selective and distinct sensitivity towards  $\text{Cd}^{2+}$  solely in presence of other metals in solution as well as in solid state.

### Crystallographic studies

From the single crystal X-ray analysis, structure of QBTP1 was determined and the ORTEP of the structure is given in Figure 7. From the crystallographic data, it is revealed that QBTP1 crystallizes in monoclinic system having space group  $P21/n$  with  $a = 11.6002$  (5) Å,  $b = 5.8523$  (2) Å,  $c = 29.8877$  (13) Å,  $Z = 4$  and  $V = 2005.33$  (14) Å<sup>3</sup>. The crystallographic data are summarised in Table S1 (SI). Some selected bond lengths and bond angles are given in Table S2 (SI).

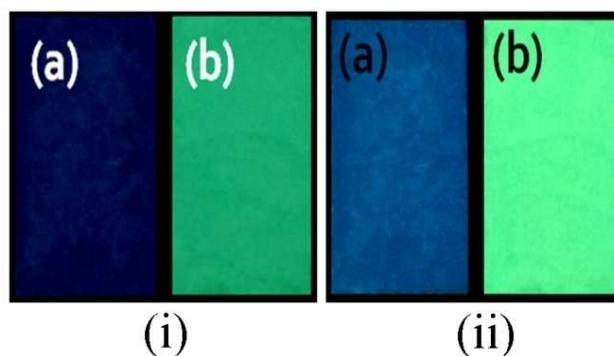


**Figure 6.** Pictures of TLC plates after immersion in methanolic solution of (i) QBTP1 and (ii) QBTP2, (a) before and (b) after addition of  $\text{Cd}^{2+}$  respectively.  $[\text{QBTP1}] = [\text{QBTP2}] = 2 \times 10^{-4}$  M,  $[\text{Cd}^{2+}] = 2 \times 10^{-3}$  M. All of the photographs are taken in UV chamber. Excitation wavelength of the UV light is 360 nm.

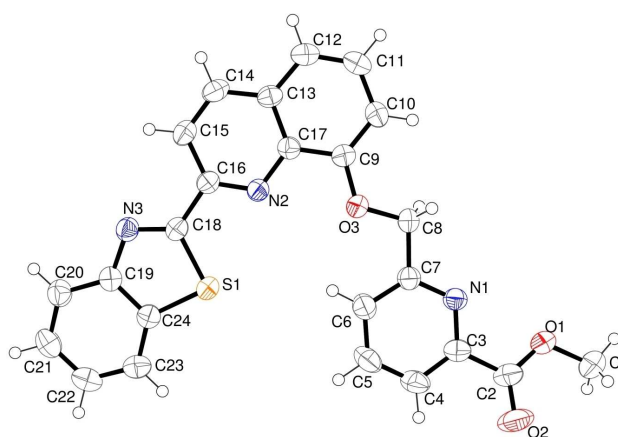


**Figure 7.** ORTEP of the probe QBTP1 showing 50% probability displacement ellipsoids for non-H atoms and the atom-numbering scheme.

### Computational Studies

We carried out density functional theory (DFT) calculations with the B3LYP/6-31 + G(d) method basis set using the Gaussian 09 program to better understand the structural changes of QBTP1 & QBTP2 upon complexation with  $\text{Cd}^{2+}$ . The optimized geometries and the highest occupied molecular orbital (HOMO) and lowest unoccupied molecular orbital (LUMO) of both the probes (QBTP1 and QBTP2) and their complexes with  $\text{Cd}^{2+}$  are shown in Figure S22-29 (SI). The HOMO-LUMO energy gap is found to be 3.86 eV and 3.87 eV for QBTP1 and QBTP2 respectively which get reduced to 3.52 eV and 2.58 eV for QBTP1- $\text{Cd}^{2+}$  and QBTP2- $\text{Cd}^{2+}$  respectively.

The ground state electronic spectra of both the probes (QBTP1 and QBTP2) and their complexes with  $\text{Cd}^{2+}$  were calculated using the time dependent density functional theory (TDDFT) using CPCM method in methanol medium. The absorption data obtained from calculation are well matched with the peaks observed experimentally (SI, Table S4-S6). For QBTP1, the transition from HOMO to LUMO, HOMO-1 to LUMO, HOMO-2 to LUMO and HOMO to LUMO+1 had contributions

mainly for the absorption peaks at 376 nm, 330 nm, 323 nm and 321 nm respectively (Table S4, SI). For QBTP1-Cd<sup>2+</sup>, main absorption peaks appeared at 404 nm, 347 nm, 343 nm and 309 nm generated from the transition of HOMO to LUMO, HOMO-1 to LUMO, HOMO-2 to LUMO and HOMO-3 to LUMO respectively (Table S4, SI). HOMO to LUMO, HOMO-2 to LUMO, HOMO-1 to LUMO and HOMO-4 to LUMO transitions for QBTP2 showed absorptions at 363 nm, 326 nm, 322 nm and 301 nm respectively (Table S6, SI). However, for CBTP2-Cd<sup>2+</sup>, the main excitation wavelengths appeared at 446 nm, 551 nm, 408 nm and 349 nm due to the transitions of HOMO to LUMO, HOMO to LUMO+1, HOMO-1 to LUMO and HOMO-1 to LUMO+1 respectively (Table S6, SI).

## Conclusions

So herein we report the fabrication of two newly developed fluorescent “turn-on” probes (QBTP1 and QBTP2) which selectively detects Cd<sup>2+</sup>. Both the probes show high selectivity towards Cd<sup>2+</sup> over other metal cations with adequately low LOD values of the order of 10<sup>-10</sup> and 10<sup>-9</sup> M respectively in physiological pH. Dipstick experiments have been performed which states that both these probes can act as a potential portable kit for detection of Cd<sup>2+</sup> in solid state as well as in solution.

## Supporting Information Summary

Supporting information consists of detailed experimental section including synthesis of the compounds and their characterizations. Detection limit calculation, association constant determination, pH study of both the compounds, quantum yield calculation, detailed crystallographic studies and computational studies along with some other spectral studies are also available in the SI.

## Acknowledgements

T.K.M thanks CSIR Govt. of India (File no. 01(0134)/19) for financial support. K.A thanks UGC (Dr. D. S. Kothari Post-doctoral fellowship, File no. CH/17-18/0224), govt. of India for providing the funding. S.G and L.P acknowledge UGC, New Delhi, India for providing them fellowships.

## Conflict of Interest

The authors declare no conflict of interest.

**Keywords:** Cd<sup>2+</sup> detection • Chemosensor • Fluorescence ‘off-on’ • ICT-CHEF • Single crystal X-ray

- [1] a) M. Waisberg, P. Joseph, B. Hale, D. Beyersmann, *Toxicology* **2003**, *192*, 95–117; b) R. K. Zalups, S. Ahmad, *Toxicol. Appl. Pharmacol.* **2003**, *186*, 163–188; c) C. C. Bridges, R. K. Zalups, *Toxicol. Appl. Pharmacol.* **2005**, *204*, 274–308.
- [2] Agency for Toxic Substances and Disease Registry, 4770 Buford Hwy NE, Atlanta, GA 30341. <http://www.atsdr.cdc.gov/cercla/07list.html>.
- [3] Cadmium in the Human Environment: Toxicity and Carcinogenicity, ed. G. F. Nordberg, R. F. M. Herber and L. Alessio, Oxford University Press, Oxford, UK, 1992.
- [4] World Health Organization, Avenue Appia 20, 1211 Geneva 27, Switzerland, [http://www.who.int/water\\_sanitation\\_health/dwq/chemicals/cadmium/en/](http://www.who.int/water_sanitation_health/dwq/chemicals/cadmium/en/).
- [5] N. Saleh, A. M. Rawashdeh, Y. A. Yousef, Y. A. Al-Soud, *Spectrochim. Acta, Part A* **2007**, *68*, 728–733.
- [6] a) R. Purkait, S. Dey, C. Sinha, *New J. Chem.* **2018**, *42*, 16653–16665; b) S. Sarkar, T. Mondal, S. Roy, R. Saha, A. K. Ghosh, S. S. Panja, *New J. Chem.* **2018**, *42*, 15157–15169; c) F. Qu, L. Zhao, W. Han, J. You, *J. Mater. Chem. B* **2018**, *6*, 4995–5002; d) M. Ghosh, S. Ta, M. Banerjee, Md Mahiuddin, D. Das, *ACS Omega* **2018**, *3*, 4262–4275; e) X. Liu, N. Zhang, J. Zhou, T. Chang, C. Fang, D. Shangguan, *Analyst* **2013**, *138*, 901–906; f) M. Li, H.-Y. Lu, R.-L. Liu, J.-D. Chen, C.-F. Chen, *J. Org. Chem.* **2012**, *77*, 3670–3673; g) J. Li, Y. Chen, T. Chen, J. Qiang, Z. Zhang, T. Wei, W. Zhang, F. Wang, X. Chen, *Sens. Actuators, B* **2018**, *268*, 446–455.
- [7] a) K. P. Divya, S. Savithri, A. Ajayaghosh, *Chem. Commun.* **2014**, *50*, 6020–6022; b) Y. Xu, L. Xiao, S. Sun, Z. Pei, Y. Pei, Y. Pang, *Chem. Commun.* **2014**, *50*, 7514–7516; c) S. Goswami, K. Aich, S. Das, A. K. Das, A. Manna, S. Halder, *Analyst* **2013**, *138*, 1903–1907; d) S. Goswami, K. Aich, S. Das, C. Das Mukhopadhyay, D. Sarkar, T. K. Mondal, *Dalton Trans.* **2015**, *44*, 5763–5770; e) K. Aich, S. Goswami, S. Das, C. Das Mukhopadhyay, C. K. Quah, H.-K. Fun, *Inorg. Chem.* **2015**, *54*, 7309–7315; f) Y. Zhang, X. Chen, J. Liu, G. Gao, X. Zhang, S. Hou, H. Wang, *New J. Chem.* **2018**, *42*, 19245–19251; g) L. Zhang, W. Hu, L. Yu, Y. Wang, *Chem. Commun.* **2015**, *51*, 4298–4301; h) Z. Shi, Q. Han, L. Yang, H. Yang, X. Tang, W. Dou, Z. Li, Y. Zhang, Y. Shao, L. Guan, W. Liu, *Chem. - Eur. J.* **2015**, *21*, 290–297.
- [8] S. Goswami, K. Aich, S. Das, A. K. Das, D. Sarkar, S. Panja, T. K. Mondal, S. K. Mukhopadhyay, *Chem. Commun.* **2013**, *49*, 10739–10741.

Submitted: May 2, 2019

Accepted: July 2, 2019